Journal of Applied Polymer Science

Modeling of Bubble-Size Distribution in Water and Freon Co-Blown Free Rise Polyurethane Foams

Debdarsan Niyogi,[1] Rajinder Kumar,[2] Kandukuri S. Gandhi[2]
[1]TATA Consultancy Services Limited, Global Consultancy Practice, Leeds, LS2 7EE, United Kingdom
[2]Department of Chemical Engineering, Indian Institute of Science, Banglore-560012, India
Correspondence to: D. Niyogi (E-mail: debdarsan.niyogi@gmail.com)

ABSTRACT: A model has been developed to simulate the foam characteristics obtained, when chemical (water) and physical (Freon) blowing agents are used together for the formation of polyurethane foams. The model considers the rate of reaction, the consequent rise in temperature of the reaction mixture, nucleation of bubbles, and mass transfer of CO_2 and Freon to them till the time of gelation. The model is able to explain the experimental results available in literature. It further predicts that the nucleation period gets reduced with increase in water (at constant Freon content), whereas with increase in Freon (at constant water) concentration nucleation period decreases marginally leading to narrower bubble-size distribution. By the use of uniform sized nuclei added initially, the model predicts that the bubble-size distribution can be made independent of the rate of homogeneous nucleation and can, thus, offer an extra parameter for its control. © 2014 Wiley Periodicals, Inc. J. Appl. Polym. Sci. **2014**, *131*, 40745.

KEYWORDS: molding; morphology; polyurethanes; theory and modeling

Received 21 November 2013; accepted 19 March 2014
DOI: 10.1002/app.40745

INTRODUCTION

Polyurethane foams are manufactured mostly by reaction injection molding (RIM). In this process, a polyol is mixed with stoichiometric amount of isocyanate, along with a catalyst, surfactant, and blowing agent(s). There are two kinds of blowing agents. Physical blowing agents are chemically inert to the reacting species, but evaporate by utilizing exothermic heat of polymerization reaction, and blow the mixture into a foam. Low-boiling chlorofluorocarbons (CFCs) fall in this class. Currently, the use of CFCs is considered to be undesirable because of its hazardous effects on the environment (ozone depletion and global warming) and many alternative physical blowing agents (cyclopentane, hydroflourocarbons, such as HCFC, HFC 365mfc, HFC 245fa, etc.) are proposed.[1–5]

The other type of blowing agent, which reacts with one of the reaction components, generating gas, is called a chemical blowing agent. Water thus acts as a chemical blowing agent for polyurethanes. Polyurethane foams are blown with mixture of water and physical blowing agent and analysis of this process is the focus of this work. In this work, water and Freon-11 combination is chosen as all the data needed to model the process are available for this system, and this enables validation against available experimental data. However, as the methodology of mathematical modeling and simulation is independent of the combination of physical and chemical blowing agents, our work will be useful in characterizing and designing other foaming processes, when all the relevant data are available, for example, in foaming by the more environmentally friendly cyclopentane investigated by Tesser et al.[6]

Polyol reacts with isocyanate to give polyurethane. The reaction is exothermic and can be represented as:

$$-\mathrm{OH} + -\mathrm{NCO} \rightarrow -\mathrm{NHCOO} - + \Delta H_{\mathrm{OH}}$$

The reaction of water (chemical blowing agent) with isocyanate is also exothermic and produces CO_2 gas. It can be written as:

$$-\mathrm{NCO} + \mathrm{H_2O} \rightarrow -\mathrm{NHCOOH} \rightarrow -\mathrm{NH_2} + \mathrm{CO_2}(g)$$
$$-\mathrm{NH_2} + -\mathrm{NCO} \rightarrow -\mathrm{NHCONH} - + \Delta H_W$$

Use of water as a chemical blowing agent provides an additional source of heat, thus raising the temperature of the reaction mixture at a faster rate. It also generates CO_2 having low solubility in the reaction mixture, thus permitting large number of nuclei to be formed. The addition of water along with freon can, therefore, provide additional control of bubble-size distribution apart from reducing gelation time. It should be mentioned that

Additional Supporting Information may be found in the online version of this article.

addition of water creates polyurea linkages that will have properties different from polyurethane linkages. The difference will depend on the functionality brought in by the amount of water added in comparison to that of polyol.

Hawkins et al.[7] investigated the relationships between cell morphology, density, and mechanical properties in a molded polyurethane material with respect to position within the mold. Their findings show that the density differences between foams alone, even after normalization, do not account for all of the variations observed in the properties. One can conclude that bubble-size distribution plays an important role in determining the foam's mechanical and thermal properties such as compressive strength, thermal conductivity, and so forth. This article focuses on determining bubble-size distribution resulting in the foaming process.

Modeling free rise foam using water and freon together has attracted the attention of research workers. Baser and Khakhar[8] proposed a model for water and freon-11 blown polyurethane foam under free-rise conditions, and in their model, they followed the same methodology of the gas–liquid equilibrium models proposed by Rojas et al.[9] and Marciano et al.[10] to handle the transport of blowing agents to vapor phase. Apart from restricting themselves to an equilibrium model of vaporization, they did not allow the concentration of CO_2 in the liquid to exceed its solubility, and the freon content in the liquid phase was assumed to be such that the temperature of the reaction mixture corresponded to the boiling point of the mixture. The solubility of carbon dioxide in the liquid phase was determined experimentally by Baser and Khakhar.[8] They obtained the kinetic parameters for the blowing reaction of isocyanate with water experimentally, assuming that they are independent of the kinetics of the reaction with polyol. The simulations based on their equilibrium model show very good agreement with their experimental data for the development of overall density profile with time. Also, the variation of temperature with time, determined experimentally, shows very good agreement with their theoretical predictions, up to the gel point.

The major limitation of foaming models that assume thermodynamic equilibrium between the vapor and liquid phase is that they can at best predict only the extent of vaporization, that is, only the density of foam. Further, as rate of vaporization has been ignored, in case a single blowing agent is used, these models can be expected to predict the maximum possible vaporization (or the smallest density attainable) at any given time. Even if one were to ignore these limitations, they can, however, lead to arbitrariness when more than one blowing agent is used. Thus, Baser and Khakhar[8] allow degassing CO_2 as soon as solubility is exceeded but do not allow vaporization of freon into CO_2 bubbles so formed by diffusion process. They assume that vaporization of freon occurs only when the temperature of the reaction mixture exceeds the boiling point of polymer-freon binary mixture. If mass tranfer processes are ignored, such arbitrariness cannot be avoided when more than a single blowing agent is used, because composition of the mixture is not uniquely determined by its boiling point. While this model is indeed very useful for predicting both temperature rise and overall foam density, as pointed out by Niyogi et al.[11] such models cannot be used to predict bubble-size distribution in the resulting foam, because they do not consider the process of nucleation and bubble growth. These are essential features of the foaming process and are important because the properties of the foam such as thermal conductivity, mechanical strength, and so forth depend strongly on the final bubble-size distribution in it.[12] Therefore, it is important to predict the bubble-size distribution in a foam as a function of its formulation.

Theoretical models for obtaining bubble-size distribution in RIM foams blown with either freon (Niyogi et al.[11]) or water (Niyogi et al.[13]) have already been reported. These authors combined the expressions for describing the reaction and thermal history with appropriate expressions for nucleation and growth of vapor bubbles. However, a different approach is required when both freon and water are present together. Here, the bubbles will contain both CO_2 and freon, and as the nuclei are formed at different times, the bubbles will differ in composition. Thus, at any time bubbles have to be characterized with respect to two parameters: size as well as composition. In this work, we account for the additional complexity arising out of this, using a more general framework which permits the calculation of the bubble-size distribution, for foams blown with a mixture of a physical and a chemical blowing agent. We also investigate, the effect of any nuclei that may initially be present in the system.

THE PHYSICAL SYSTEM AND ASSUMPTIONS

Free-rise foaming, when both chemical (water) and physical (freon) blowing agents are present is considered. The mold is filled partially with a mixture of polyol, isocyanate, small amount of catalyst, surfactant, and blowing agents. Polymerization reaction between isocyanate and polyol as well as reaction of isocyanate with water to produce CO_2 take place. As both the reactions are exothermic, the temperature of the mixture rises. At a certain time, when the sum of the partial pressures exerted by CO_2 and freon exceeds the total pressure of the system, the solution becomes supersaturated. Nucleation occurs when supersaturation builds to a suitably high value. The time at which the first nuclei are born is referred to as cream time. Foaming begins when these nuclei grow by diffusion of freon and CO_2 from the liquid phase into the bubble phase. Nucleation continues till the supersaturation becomes negligible. For some time, nucleation and bubble growth occur simultaneously, generating a bubble-size distribution, which needs to be predicted.

Modeling assumptions for free-rise foaming have been discussed and justified elsewhere (Niyogi et al.[11]) in detail. We briefly restate them here.

1. The mold is assumed to be a cylindrical cup of uniform cross section to facilitate comparison with the results of Baser and Khakhar.[8]
2. Simulation is carried out till the gel point is reached at which stage the bubble-size distribution gets frozen.
3. Nucleation is assumed to be homogeneous.
4. Adiabatic conditions are assumed.

5. It is assumed that there is no coalescence of bubbles and that no relative motion exists between the bubbles and the liquid. Jung et al.[14] studied PUF blown by HCFC and water. They suggested that the observed increase in the bubble size with an increase of initial blowing agent concentration was due to coalescence. Two factors other than coalescence also affect the bubble size. As more amount is available, increased initial blowing agent concentration will lead to increased bubble size if nuclei born remain constant. However, number of nuclei born can also increase, which can reduce the bubble size. Kim et al.[15] reported that liquid-type silane additives lower the surface tension, prohibit the coalescence of bubbles, and promote formation of small dense cells. In a similar fashion, Seo et al.[16] reported that the cell size of the PUF samples decreased from 360 to 146 μm with an increase in surfactant from 0 to 0.33 php, respectively, indicating prevention of coalescence. Although coalescence cannot be neglected altogether, it is to be noted that the phenomenon depends largely on the nature and concentration of the surfactant used. Thus, the results obtained assuming absence of coalescence will form a limiting case and also give an estimate of the smallest mean size that can be obtained in an experiment.
6. Liquid-to-gas-mass transfer is assumed to be purely diffusional and controlled by the liquid-side resistance.
7. Gas phase is assumed to behave ideally.
8. It is assumed that neither polymer nor monomers evaporate.
9. Evaporation of water into gas phase is neglected as it is present in a very low concentration and also gets quickly consumed by the blowing reaction.
10. All physical properties are assumed to be constant and volume changes due to mixing in liquid phase are neglected.

MATHEMATICAL FORMULATION

The energy balance equation is solved simultaneously with the reaction kinetics of the polymerization reaction, the kinetics of the blowing reaction, and the rates of diffusion of CO_2, and freon to the gas phase. Normally, bubble-size distribution is obtained by solving the population balance equation which is coupled with the system of equations through the rate of increase of the mass of blowing agent in the gas phase. As there are two blowing agents, it is possible that bubbles of different age will contain different mole fractions of CO_2 and freon. Thus, bubble size as well as composition of gas phase change with time and have to be taken into account. The set of governing equations becomes quite complex, necessitating an elaborate numerical procedure for obtaining bubble-size distribution. These steps are discussed in detail in the following sections.

Energy Balance

The temperature of the system rises because of the heat generated by the two exothermic reactions (viz., polymerization and the blowing reaction). The rise in the temperature is reduced as part of the heat generated is utilized by the evaporation of the physical blowing agent. Hence, considering the sensible heat required in raising the temperature of the liquid phase as well as the gas phase, the unsteady energy balance is written as:

$$\left[m_p C_{p_p} + m_{\mathrm{CO}_2,g} C_{p_{\mathrm{CO}_2,g}} + m_B C_{p_B} + m_{B,g} C_{p_{B,g}}\right] \frac{dT}{dt} = (-\Delta H_{\mathrm{OH}}) C_{\mathrm{OH}_0} \frac{dX_{\mathrm{OH}}}{dt} + (-\Delta H_W) C_{W_0} \frac{dX_W}{dt} + \lambda \frac{dm_B}{dt} \quad (1)$$

The kinetic parameters for polymerization and blowing reactions determined, assuming that they are independent of each other, by Baser and Khakhar[8] are used here. These investigators absorbed the latent heat of vaporization of CO_2 in the heat of reaction of water and isocyanate. Therefore, the former is not included in the energy balance equation, because we use the values for parameters given by them. To solve the above equation, expressions for the kinetics of the reactions, rate of evaporation of blowing agent, and rate of diffusion of CO_2 into the vapor phase are required. These are discussed later.

Kinetics

Baser and Khakhar[8] reported the kinetic parameters for both polymerization and blowing reaction and the same are used here. The rates of the reactions get lowered because of the dilution effect caused by addition of physical blowing agent. The dilution terms account for this. The dilution terms given by them have been recast here for convenience.

Polymerization Rate

Polymerization reaction follows a second-order kinetics:

$$\frac{dX_{\mathrm{OH}}}{dt} = A_{\mathrm{OH}} \exp\left[-\frac{E_{\mathrm{OH}}}{RT}\right] C_{\mathrm{OH}_0}(1-X_{\mathrm{OH}}) (r_{\mathrm{NCO}} - 2r_W X_W - X_{\mathrm{OH}}) \left[(1-W_B)\frac{\rho_L}{\rho_p}\right] \quad (2)$$

where,

$$r_{\mathrm{NCO}} = C_{\mathrm{NCO}_0}/C_{\mathrm{OH}_0} \quad (3)$$

$$r_W = C_{W_0}/C_{\mathrm{OH}_0} \quad (4)$$

$$X_{\mathrm{OH}} = (C_{\mathrm{OH}_0} - C_{\mathrm{OH}})/C_{\mathrm{OH}_0} \quad (5)$$

Blowing Reaction Rate

The reaction of isocyanate with water is given by a first-order reaction kinetics:

$$\frac{dX_W}{dt} = A_W \exp\left[-\frac{E_W}{\mathrm{RT}}\right](1-X_W)\left[(1-W_B)\frac{\rho_L}{\rho_p}\right] \quad (6)$$

$$X_W = (C_{W_0} - C_W)/C_{W_0} \quad (7)$$

The liquid-phase density (ρ_L) at any instant of time is expressed as:

$$\rho_L = \frac{m_p + m_W + m_B}{\frac{m_p}{\rho_p} + \frac{m_W}{\rho_W} + \frac{m_B}{\rho_B}} \quad (8)$$

Rate of Blowing Agent Diffusion/Evaporation

The rate of mass transfer of CO_2 and freon into a bubble of diameter l is given by:

$$N_{\mathrm{CO}_2}(l) = k_m \pi l^2 \left(C_{\mathrm{CO}_2} - C^*_{\mathrm{CO}_2}\right) = k_m \pi l^2 \Delta C_{\mathrm{CO}_2} \quad (9)$$

$$N_B(l) = k_m \pi l^2 \left(C_B - C^*_B\right) = k_m \pi l^2 \Delta C_B \quad (10)$$

C^*_B and $C^*_{\mathrm{CO}_2}$ are the liquid-phase concentrations at the vapor–liquid interface and are in equilibrium with the vapor phase as liquid-side resistance controls mass transfer. Thus, they are

dependent on the vapor composition. In general, N_B and N_{CO_2} will not always be in a constant proportion and hence, the bubble composition will change with time. This in turn will alter the values of C_B^* and $C_{CO_2}^*$. Clearly, the degassing of CO_2 and vaporization of freon are coupled and cannot be assumed to occur independently. Further, it is important to note that driving forces for mass transfer are different for bubbles of different sizes.

All bubbles born at a given time would grow with identical histories, and hence would have the same size, composition, and so forth. Thus, a single parameter is sufficient to characterize the population of bubbles. It is chosen to be the diameter of the bubble for convenience.

If $f(l)dl$ is defined as the number of bubbles per unit volume of liquid phase in size range between l and $l+dl$, the rate of increase of mass of CO_2 in the gas phase and the depletion of freon in the liquid phase can be written as:

$$\frac{dm_{CO_2,g}}{dt} = \int_{l_N}^{l_{max}} M_{CO_2}[N_{CO_2}(l)f(l)V_L]dl \tag{11}$$

$$-\frac{dm_B}{dt} = \int_{l_N}^{l_{max}} M_B[N_B(l)f(l)V_L]dl \tag{12}$$

Here for the sake of simplicity, the mass-transfer coefficient has been assumed to be the same for both components. The differences can be accounted for but at the expense of increased computational complexity. The mass-transfer coefficient for liquid-phase diffusion controlled process is given by eq. (24) and will be discussed a little later.

To complete the calculation of the rate of mass transfer of CO_2 and freon from the above equations, the driving forces for mass transfer and the bubble-size distribution have to be computed. The latter in turn depend on the nucleation and growth, and these are discused later. Subsequently, we describe the method for computing the driving forces.

Nucleation Rate

Following Niyogi et al.,[11] the vapor pressure exerted by freon can be calculated once its activity coefficient is known:

$$\gamma_B(T,W_B)W_BP^{sat}(T) = P_{V_B} \tag{13}$$

The above equation relates the weight fraction of a solute in the polymer to the vapor pressure exerted by it, when thermodynamic equilibrium prevails at the interface. It needs a model for or data on activity coefficients. Model free approaches to predict information equivalent to eq. (13) from data have been proposed by Li et al.[17] However, this approach requires data on solubility of freon vapor in polyurethanes and that information is not available. Hence, we resort to use of eq. (13) after making suitable assumptions.

We assume the partial pressure exerted by CO_2 to follow Henry's law and the Henry's law coefficient is not influenced by the presence of freon. Hence, the values of Henry's law coefficient calculated from the solubility of CO_2 reported by Baser and Khakhar[8] (see Table IV) have been used here. The total vapor pressure exerted by the liquid phase is given by the sum of the partial pressures exerted by freon and CO_2:

$$P_V = HC_{CO_2} + \gamma_B(T,W_B)W_BP^{sat}(T) \tag{14}$$

Nucleation begins once P_V exceeds the system pressure P_L, and the rate depends on the difference between the two. In view of paucity of data, we implement the above scheme after making a few simplifications. We assume that the saturation vapor pressure exerted by freon is unaffected by the presence of carbon dioxide and water. This is justifiable as, usually, the amount of water added to, and the CO_2 present in the liquid phase are very small. The activity coefficient of freon in the liquid phase depends on both the temperature and weight fraction of freon. Of these, we assume that weight fraction is the dominant variable. As we shall show now, this allows prediction of activity coefficients from the data of Marciano et al.[10] They reported normal boiling points of binary liquid mixtures as a function of weight fraction of freon. The activity coefficients in the liquid phase were calculated from the normal boiling point data as follows:

$$\gamma_B(T^*(W_B),W_B)W_BP^{sat}(T^*(W_B)) = P = 1\ \text{atmosphere} \tag{15}$$

where $T^*(W_B)$ is the boiling point of the binary liquid mixture in which the weight fraction of freon is W_B. The assumption that the activity coefficient is dominated by composition implies that $\gamma_B(T,W_B)$ and $\gamma_B(T^*(W_B),W_B)$ is equal. Thus, the partial pressure exerted by freon is calculated from

$$\gamma_B(T^*(W_B),W_B)W_BP^{sat}(T) = P_{V_B} \tag{16}$$

Expression for $T^*(W_B)$ was given by Marciano et al.[10]

$$W_B = \frac{0.314}{\exp[(2980-10.034T^*(W_B))/(191.22-T^*(W_B))]-0.686} \tag{17}$$

In the temperature range of interest, $P^{sat}(T)$ is evaluated using Antoine equation:

$$P^{sat}(T) = exp[\text{Ant } A - \text{Ant } B/(T+\text{Ant } C)] \tag{18}$$

$\gamma_B(T^*(W_B),W_B)$ was calculated using eq. (15) after evaluating $P^{sat}(T^*(W_B))$ using eq. (18).

In summary, the total vapor pressure exerted by the liquid phase is given by the sum of the pressures exerted by freon and CO_2:

$$P_V = HC_{CO_2} + \gamma_B(T^*(W_B),W_B)W_BP^{sat}(T) \tag{19}$$

and was evaluated from eq. (19) at any given time.

The expression for nucleation rate (J) used according to the classical nucleation theory is:

$$J = M\,B\,exp\left[\frac{-\Delta F^*}{nkT}\right] \tag{20}$$

where,

$$\Delta F^* = \frac{16\pi\sigma^3}{3(P_V-P_L)^2} \tag{21}$$

Here, M denotes the total number of molecules of freon and CO_2 in the liquid phase. The frequency factor B is treated as an adjustable parameter due to the lack of experimental data.

Growth Rate

The growth rate $G(l)$ of a bubble of size l is obtained from the mass balance equation, assuming the vapor phase to be ideal:

$$\frac{d}{dt}\left[\frac{\pi}{6}l^3\frac{P}{\mathrm{RT}}\right]=N_{\mathrm{CO}_2}(l)+N_B(l)=k_m\pi l^2\left[(C_B-C_B^*)+(C_{\mathrm{CO}_2}-C_{\mathrm{CO}_2}^*)\right] \tag{22}$$

$$\frac{dl}{dt}=G=\frac{2k_m\mathrm{RT}\,(\Delta C_{\mathrm{CO}_2}+\Delta C_B)}{P}+\frac{l}{3T}\frac{dT}{dt} \tag{23}$$

As aforementioned, it is important to note that driving force depends on size of the bubble.

Mass-Transfer Coefficient

The liquid to gas mass-transfer coefficient k_m is considered to be purely diffusional and controlled by liquid side resistance. For a spherical bubble of size l, Sherwood number can be taken as two and, thus, k_m becomes

$$k_m=\frac{2D}{l} \tag{24}$$

The diffusion coefficient D is assumed to be constant. Once again, it is possible to take into account the variation of diffusion coefficient with the degree of polymerization and has not been undertaken to keep the model computationally simple.

Substituting for k_m in eq. (23), the growth rate becomes:

$$G=\frac{dl}{dt}=\frac{4\mathrm{RTD}\,(\Delta C_{\mathrm{CO}_2}+\Delta C_B)}{Pl}+\frac{l}{3T}\frac{dT}{dt} \tag{25}$$

Bubble-Size Distribution

For the case, where both chemical and physical blowing agents are present, simultaneous degassing and evaporation of the blowing agents take place. Therefore, each bubble will contain a mixture of gaseous freon and carbon dioxide. In the absence of coalescence, each bubble will interact only with the surrounding liquid. Hence, bubbles born at the same time will have the same composition at any instant. However, the composition will be different for bubbles grown of nuclei born at a different time. Hence, here we have to compute the composition and the bubble size as a function of time. As the equilibrium concentrations of freon and carbon dioxide at the gas–liquid interface depend on the vapor composition, it is readily appreciated that both C_B^* and $C_{\mathrm{CO}_2}^*$ will be functions of bubble size. This means that the driving force for the liquid to gas mass transfer will be different for bubbles born at different times, thus having unequal ages and sizes. Analytical solution for a population balance equation that incorporates all these effects could not be found, and a numerical approach is followed here. In this approach, beginning with the first instance of nucleation, the bubbles born during each successive small period of time Δt are grouped into different sets indexed by the time interval in which they are born after the cream time. As the value of Δt is sufficiently small, it is assumed that within a single set, the bubbles will experience the same kind of external conditions throughout, and thus, have the same size. During time interval Δt, the number of nuclei formed at any given time t is given by $J(t)V_L\Delta t$. As coalescence is absent, if there are K such sets at any time t, the ith set contains $n_{b,i}$ number of bubbles given by the equation

$$n_{b,i}(t)=n_{b,i}(t_c+i\Delta t)=J(t_c+i\Delta t)V_L\Delta t \quad i=1,..K\ t\geq t_c+K\Delta t \tag{26}$$

where t_c is the cream time. K increases by unity as long as nucleation occurs during the current time interval, and remains constant otherwise. Since the number and size for each set of bubbles are known, at any instant of time, the moments of the distribution can be calculated as follows:

$$f_0V_L=\sum_{i=1}^{K}n_{b,i} \tag{27}$$

$$f_1V_L=\sum_{i=1}^{K}n_{b,i}l_i \tag{28}$$

$$f_2V_L=\sum_{i=1}^{K}n_{b,i}l_i^2 \tag{29}$$

$$f_3V_L=\sum_{i=1}^{K}n_{b,i}l_i^3 \tag{30}$$

The mass balance for freon and CO_2 can be written as:

$$-\frac{dm_B}{dt}=\sum_{i=1}^{K}2\pi DM_Bn_{b,i}l_i\Delta C_{B,i} \tag{31}$$

$$\frac{dm_{\mathrm{CO}_2,g}}{dt}=\sum_{i=1}^{K}2\pi DM_{\mathrm{CO}_2}n_{b,i}l_i\Delta C_{\mathrm{CO}_2,i} \tag{32}$$

The above are discrete versions of eqs. (11) and (12). To use the above two equations, it is necessary to calculate the size of the ith set of bubbles at any time.

Equation (25), can be written for each set i, and rearranged as:

$$\frac{d\left(l_i^2T^{-2/3}\right)}{dt}=\frac{dY}{dt}=\frac{8\mathrm{RT}^{1/3}D(\Delta C_{B,i}+\Delta C_{\mathrm{CO}_2,i})}{P} \tag{33}$$

Initial condition for this equation is given by:

$$\text{at}\quad t=r_i,\quad Y=l_N^2T^{-2/3}(r_i) \tag{34}$$

where r_i represents the time of birth of ith set of bubbles. Integrating,

$$l_i^2T^{-2/3}(t)-l_N^2T^{-2/3}(r)=\int_{t'=r}^{t'=t}\frac{8\mathrm{RT}^{1/3}(t')D\left(\Delta C_{\mathrm{CO}_2,i}(t')+\Delta C_{B,i}(t')\right)}{P}dt' \tag{35}$$

Thus, the size of the ith set of bubbles at any instant of time is calculated using the above equation.

Calculation of $C_{B,i}^*$

As the equilibrium concentrations of freon and CO_2 ($C_{B,i}^*$ and $C_{\mathrm{CO}_2,i}^*$) at the gas–liquid interface will depend on the gas-phase compositions, for each set of bubbles the mole fractions of freon and CO_2 in the vapor phase, $y_{B,i}$ and $y_{\mathrm{CO}_2,i}$, are to be determined. The following relationships have to be satisfied at all times:

$$\gamma_B(T^*(W_{B,i}^*),W_{B,i}^*)W_{B,i}^*P^{\mathrm{sat}}(T)=y_{B,i}P \tag{36}$$

$$y_{\mathrm{CO}_2,i}=1-y_{B,i} \tag{37}$$

$$C_{\mathrm{CO}_2,i}^*H=y_{\mathrm{CO}_2,i}P \tag{38}$$

After the required supersaturation is reached, $J>0$. Let, the number of moles in the nuclei be zero but let the mole fraction of freon in the nuclei be

Table I. Properties of the Reactants

Reactant	Property	Reference
Polymethylenepolyphenyl isocyanate	Equiv. wt. 135	Baser and Khakhar[8]
Polyetherpolyol (SU-365)	OH No. 365 mg KOH/g polyol	

$$y_{B,N} = \frac{P_{V_B}}{P_V} = \frac{\gamma_B(T^*(W_B), W_B) W_B P^{\text{sat}}(T)}{P_V} \tag{39}$$

So, for nuclei, knowing $y_{B,N}$ the eq. (36) is solved iteratively for a value of $W^*_{B,N}$.

In the next time step, for ith set of bubbles growing the gas-phase composition with respect to freon is given by

$$y_{B,i} = \frac{N_{R,i}}{N_{R,i}+1} \tag{40}$$

where, $N_{R,i}$ is the ratio of number of moles of freon to that of CO_2 in the vapor phase of ith set of bubbles. The value of $N_{R,i}$ is calculated by integrating mass transport eqs. (31) and (32). Thus, knowing $y_{B,i}$, $W^*_{B,i}$ is calculated iteratively in the same manner as before.

$C^*_{B,i}$ is calculated from $W^*_{B,i}$ as follows:

$$C^*_{B,i} = \frac{W^*_{B,i}(m_p + m_B + m_W)}{(V_L M_B)} \tag{41}$$

Now eqs. (1), (2), (6), (27–32), and (35) are to be solved simultaneously. The overall foam density can be calculated from these results by the following equation:

$$\rho_{\text{all}} = \frac{m_p + m_{W_0} + m_{B_0}}{\frac{(m_{B_0} - m_B)\text{RT}}{\text{PM}_B} + \frac{m_{\text{CO}_2,g}\text{RT}}{\text{PM}_{\text{CO}_2}} + \frac{m_p}{\rho_p} + \frac{m_B}{\rho_B} + \frac{m_W}{\rho_W}} \tag{42}$$

PARAMETERS FOR COMPUTATION

Two foam formulations are chosen for simulation to compare with the experimental data of Baser and Khakhar.[8] Here, the initial weight percentages of water and freon are expressed with respect to the weight of polyol taken. Four other initial compositions are also simulated to study the effect of initial percentages of blowing agents on the bubble-size distribution. The data used for simulations are given in Tables I to V.

NUMERICAL SIMULATION

The set of ordinary differential equations is solved by an International Mathematics and Statistics Library (IMSL) subroutine following Adams–Moulton method. Initially, only energy balance and kinetic equations are solved, till the point is reached when the liquid-phase vapor pressure P_V is greater than one atmosphere and the nucleation rate is greater than zero. Now for each time step, the following procedure is repeated. The number of bubbles born during the time step is evaluated using eq. (26) where Δt stands for the value of the time step currently being tried by the IMSL routine internally. Next, a trial and error solution is sought to yield converged values of $W^*_{B,i}$ for each set of bubbles to get the values of $\Delta C_{B,i}$ and $\Delta C_{\text{CO}_2,i}$, as described earlier. Now with these values of $\Delta C_{B,i}$ and $\Delta C_{\text{CO}_2,i}$, the depletion of the blowing agents in the liquid phase are obtained from eqs. (31) and (32). When nucleation comes to a halt, the total number of sets of bubbles becomes fixed. However, the convergence procedure is still carried out to evaluate the rates of mass transfer of the blowing agents till the gel point is reached.[18]

RESULTS AND DISCUSSION

The only adjustable parameter in the present model, namely, the frequency factor for the nucleation rate (B) is tuned to match the experimental density profiles of Baser and Khakhar[8] (Table V). All the graphs are plotted till the gel point ($X_{\text{OH,gel}} = 0.5$).

Variation of Bulk Temperature with Time

The bulk temperature is plotted versus time in Figure 1 with the experimental data of Baser and Khakhar[8] and model simulations. It is seen that simulations of both models agree well with the experimental data. The temperature curve is steeper for more water and less freon content in the mixture. As the system can be considered practically adiabatic, the temperature of the foam increases due to the two exothermic reactions (viz., polymerization and blowing reaction), and the tendency for the temperature to decrease is due to evaporation of freon. The blowing reaction is first order with respect to the concentration

Table II. Physical Property Data

Property	Species	Symbol	Value	Unit	Reference
Density	Polymer	ρ_p	1100.0	kg/m^3	Baser and Khakhar[8]
	Freon	ρ_B	1467.0		
Specific heat	Polymer	C_{p_p}	1800.0	J/kg K	
	Freon (vap)	$C_{p_{B,g}}$	593.0		
	Freon (liq)	C_{p_B}	870.0		
	CO_2 (gas)	$C_{p_{\text{CO}_2,g}}$	836.6		
Latent heat of vaporization	Freon	λ	2.0×10^5	J/Kg	
Molecular weight	Freon	M_B	137.37	Kg/Kmol	
Diffusivity	Freon and CO_2	D	1×10^{-9}	m^2/s	
Surface tension	Mixture	σ	0.027	N/m	

Table III. Initial Concentrations of Water and Freon

Blowing agent (s)	% Water	% Freon (R11)	$T_0(K)$
Water and Freon	1.0	10.0	303
	1.0	15.0	303
	1.0	27.0	303
	1.0	27.0	299
	3.0	10.0	303
	3.0	15.0	303
	3.0	27.0	303

of water. So the rate of rise of temperature will be faster for greater initial water content. Simultaneously, lower initial concentration of freon also results in faster rates of reaction due to the lesser effect of dilution as well as lesser consumption of heat due to slower rates of evaporation. Therefore, a higher rate in rise of temperature is observed for an initial composition of 3% water and 10% freon than with 1% water and 27% freon. Although the simulation curve for this model shows a good match with the experimental values for 3% water and 10% freon, that for 1% water and 27% freon predicts a slower rate of rise. The simulations of Baser and Khakhar[8] show good agreement with the experimental data. Both the models show a slight kink, though the present model shows it earlier. The kink is the result of sudden utilization of heat due to bubble growth. This happens in the case of model of Baser and Khakhar,[8] when the boiling point of freon is reached, whereas in the present model it occurs as soon as nucleation begins which is earlier.

To characterize the effect of initial weight fraction of freon on the rate of rise of temperature, the temperature was computed as a function of time for several other combinations of $W_{W,0}$ and $W_{B,0}$ for the same initial temperature of 303 K for all cases. It was found that the bulk temperature increases more rapidly as the freon concentration decreases for the same initial weight fraction of water (Figure 2). This is because of higher evaporation with increased freon produces an enhanced cooling effect on the system. Further, the greater the initial concentration of freon, the slower is the rate of reaction due to dilution effect. As blowing reaction is faster than polymerization, temperature rise is more sensitive to $W_{W,0}$ than $W_{B,0}$. Thus, the two were nearly compensating and initial concentrations combinations of 1% water, 10% freon and 3% water, 27% freon, gave results very close to each other.

Conversions of Polyol and Water

Fractional conversions of polyol X_{OH}, follow curves (not shown) similar to that of Figure 2 due to the fact that kinetics are largely tied together with the temperature rise rates. Calculation of the fractional conversions of water X_W indicate that in all the cases, water is almost fully reacted within about 3 min.

Rise Time

Rise time t_r, the time taken for the foaming mixture to achieve full height when it turns to a soft gel, is shown in Figure 3 with respect to the initial weight fraction of freon, and $W_{W,0}$ as parameter. Roughly a linear increase is seen as we move on to higher $W_{B,0}$ for the same initial concentration of water, and a higher rise time for lower $W_{W,0}$, for the same initial weight fraction of freon. These trends are expected in view of dilution effects for higher $W_{B,0}$ and higher temperature rise rate for higher $W_{W,0}$.

Concentration of Freon and CO_2 in the Liquid Phase

As will be seen a little later, the period of nucleation is found to be very short. During this short time period, the concentration of freon remains nearly constant, whereas that of CO_2 passes through a maximum. This is shown in Figure 4. The increase is due to generation of CO_2, whereas the decrease is due to mass transport to growing bubbles. The figure displays two more interesting features. With 3% water, the build up of CO_2 concentration is much higher than for 1% water. With higher freon concentration, the CO_2 build up is not only lesser but also falls earlier for both the concentrations of water. These features are the result of intricate interplay of the rate of formation of CO_2,

Table IV. Thermodynamic and Kinetic Data

Parameter	Symbol	Value	Unit	Reference
Heat of reaction	$-\Delta H_{OH}$	7.075×10^7	J/k equiv	Baser and Khakhar[8]
	$-\Delta H_W$	8.6×10^7	J/k mol	
Chemical conversion at gel point	$X_{OH,gel}$	0.5		
Activation energy for chemical reaction	E_{OH}	4.04×10^7	J/k mol	
	E_W	3.266×10^7		
Frequency factor	A_{OH}	1.7348×10^3	m^3/k equiv/s	
	A_W	1.385×10^3	s^{-1}	
Antoine Constants (Freon)	*AntA*	15.8516	N/m^2, K	
	AntB	2401.61		
	AntB	−36.3		
Amount of CO_2 soluble in Polymer per unit polymer mass	$(CO_2)_D$	4.4×10^{-4}		Baser and Khakhar[8]

Table V. Model Parameters

Parameter	Symbol	Value	Unit
Frequency factor in nucleation rate expression	B	1×10^{-10}	s^{-1}
Critical nucleus size	l_N	0.4×10^{-6}	m

the rate of nucleation, and the rate of mass transport of CO_2 and freon into the nucleated bubbles. The high water concentrations (at a fixed freon content) yield very high rates of build up of CO_2 concentration because of fast reaction. As a result, the rate of nucleation is also high and the decrease of CO_2 concentration occurs quickly due to mass transfer to a large number of nuclei, to which both CO_2 and freon diffuse. With increased freon concentration (at a fixed water content), the rate of reaction is slower due to dilution effect. Nucleation occurs at an earlier time (as will be shown later on) but the area for the mass transport increases rapidly because the bubble growth is faster due to higher freon concentration. As a result, concentration of CO_2 falls at an early time.

As the freon concentrations do not change much during the short time over which nucleation occurs, it may also be concluded from Figure 4 that formation of CO_2 has a dominant effect on the onset of nucleation and initial growth of bubbles.

Nucleation Rate

Nucleation in presence of both water and freon is much more complex than when only one of them is present. This is because freon can add to supersaturation and also have the opposite effect through dilution.

To illustrate this, let us consider the profiles for partial pressures of freon ($P_{V,B}$) and that of CO_2 (P_{V,CO_2}) as depicted in Figures 5 and 6, respectively. For a constant water concentration, $P_{V,B}$ increases with increase in freon concentration, as expected. For a higher water concentration, since larger number of bubbles are formed at an earlier time, partial pressure of freon is lower due to its increased diffusion rate. A kink is observed at an earlier time in all of the curves, which is due to sudden increase in evaporation of Freon at the incipient of nucleation.

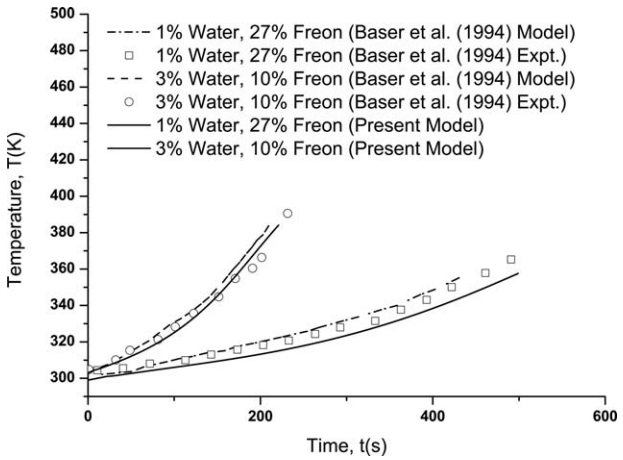

Figure 1. Variation of bulk temperature with time for two different initial weight fractions of freon and water.

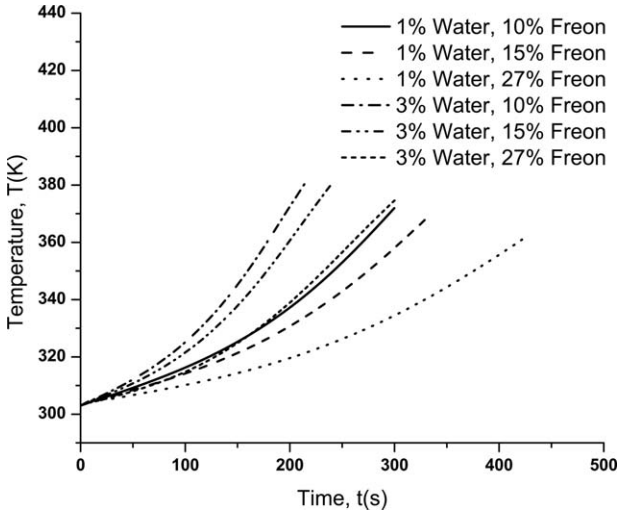

Figure 2. Variation of bulk temperature with time for six different initial weight fractions of freon and water.

The profile of P_{V,CO_2} is shown in Figure 6. It is apparent that for higher initial water concentration, more is the generation of CO_2, leading to its higher partial pressure. For a particular water concentration, with increase in freon concentration, the steepness of the curve decreases slightly due to the dilution effect. Also, the peak of P_{V,CO_2} curve is decreased for higher initial freon concentration. This suggests more degassing of CO_2 is taking place. This can be explained based on higher mass transfer of freon leading to formation of larger bubble sizes, more surface area for mass transfer and, thus, suppression of buid up of P_{V,CO_2}. The curves are narrower for higher initial Freon concentration at a constant water percentage because of the same reason.

The total vapor pressure P_V, which is a sum of P_{V,CO_2} and $P_{V,B}$ is plotted against time in Figure 7. It can be seen that its features are dominated by CO_2. The resultant effect of individual

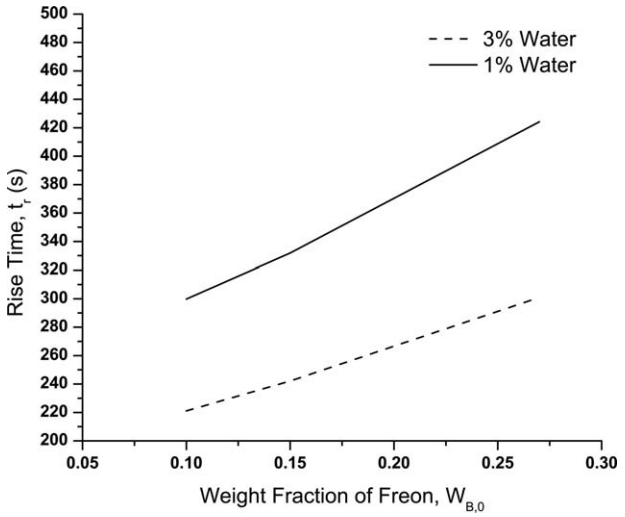

Figure 3. Variation of rise time for different initial concentrations of freon and water.

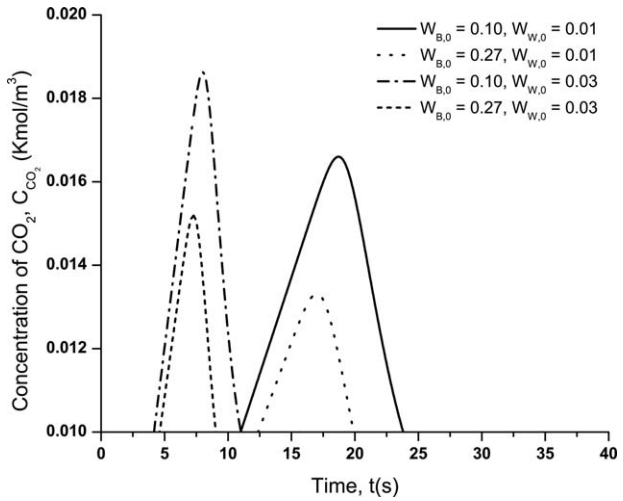

Figure 4. Variation of carbon dioxide concentration in the bulk liquid with time.

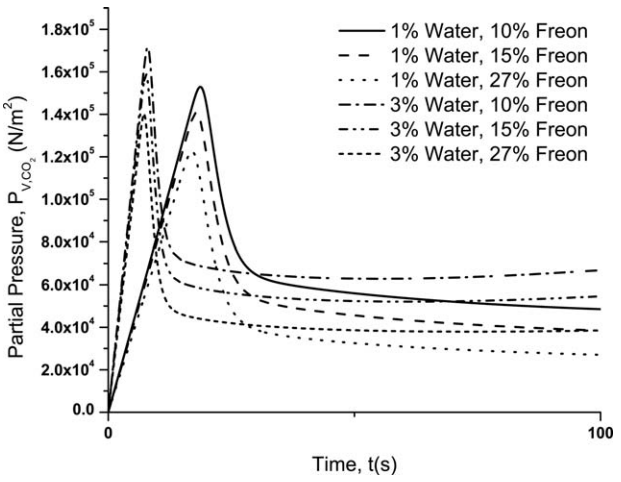

Figure 6. Variation of partial pressure of carbon dioxide with time.

partial pressures is twofold – one is with increase in water percentage, the rate, and peak of the curves are higher, whereas the other is that with increase of freon concentration, the building up of P_V happens earlier, and a lower peak value is attained.

Figure 8 shows the nucleation rate for six different initial concentrations of blowing agents. The nucleation rate depends mainly on two factors. One is how fast the reaction mixture gets supersaturated with the blowing agents to initiate nucleation, and the other is the rapidity with which the blowing agents are diffusing/evaporating into the gas phase. Here, as seen earlier, higher percentage of water results in a steeper temperature rise, which in turn induces a faster achievement of supersaturation required for nucleation, both due to evolution of CO_2 and rise in temperature. So for the formulations containing 3% water, nucleation begins earlier than for the ones with 1% water. Further, the peak is greater for the former as the amount of water, and hence CO_2 generated, is more. It is seen that the width of nucleation curve decreases with increase in water percentage. Here, as the water content is

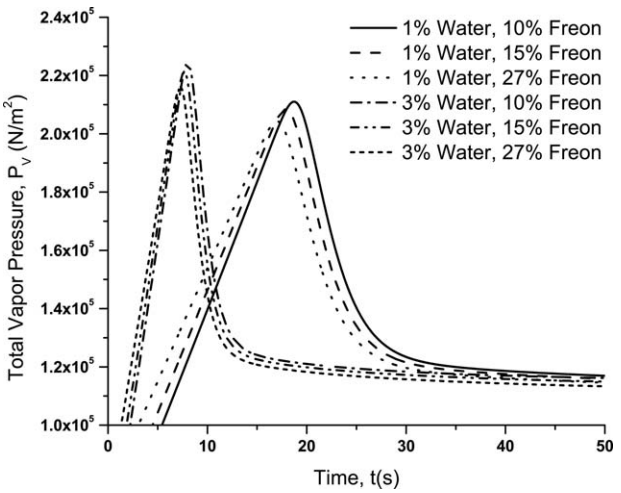

Figure 7. Variation of total vapor pressure with time.

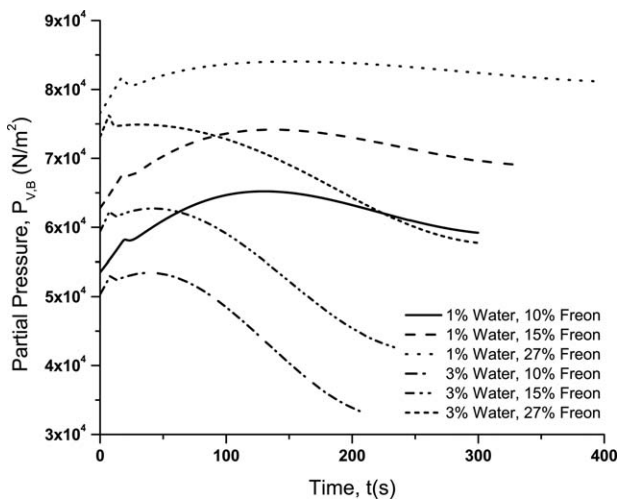

Figure 5. Variation of partial pressure of freon with time.

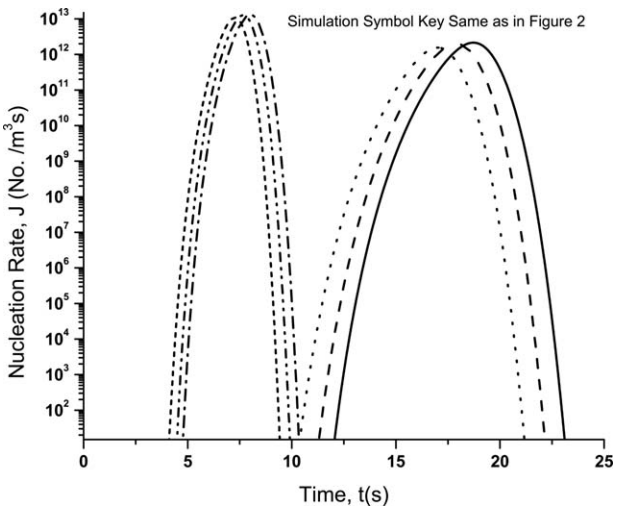

Figure 8. Variation of nucleation rate with time.

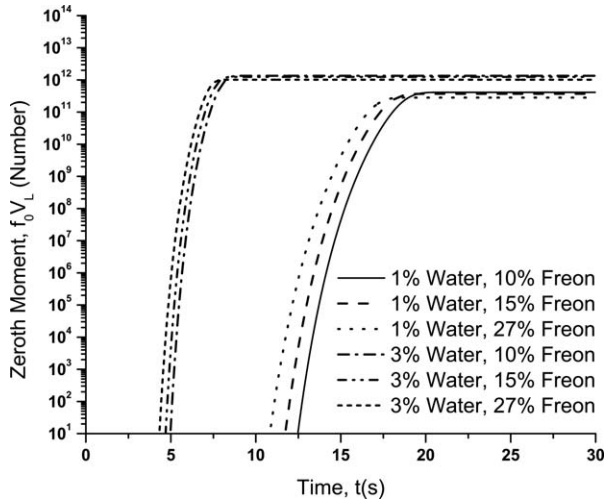

Figure 9. Variation of zeroth moment with time.

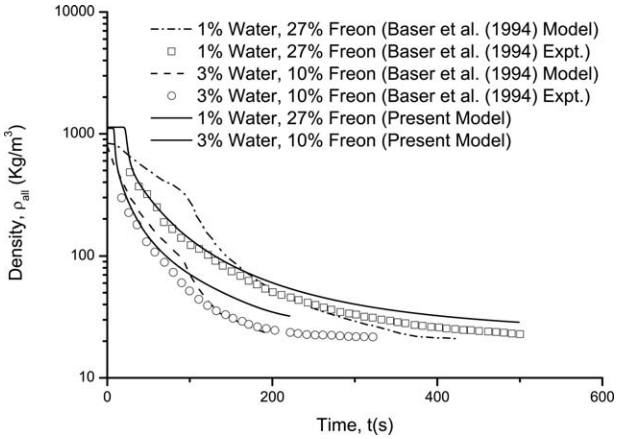

Figure 11. Variation of overall foam density with time for two different freon and water concentrations.

increased, as seen earlier, nucleation rate is greater. This implies that the number of nuclei produced are greater. Thus, one would expect greater rate of mass transfer. This would then tend to bring down the supersaturation quickly or reduce the time interval of nucleation. However, as CO_2 produced is more, higher amount of CO_2 has to diffuse into the vapor phase to reduce the supersaturation. This would, therefore, tend to increase the time period of nucleation. The rate of nucleation for higher water content is greater because of the nonlinear dependence of nucleation rate on CO_2 concentration. Therefore, even though there is more CO_2 generated in case of 3% water content, there are a much larger number of bubbles into which this excess CO_2 can diffuse into. As a result, the time period over which nucleation occurs decreases with increased water content.

When the amount of freon present is increased keeping the amount of water constant, it is observed that nucleation occurs over slightly larger period of time. Conversely, for higher $W_{B,0}$, the peak of nucleation rate curve is slightly higher. This is to be expected as nucleation rate curves would follow the same pattern as the profile of total vapor pressure P_V (Figure 7), the latter being indicative of the degree of supersaturation.

Number of Bubbles Formed

Zeroth moment ($f_0 V_L$) is drawn versus time in Figure 9. The Figure shows that the zeroth moment, which represents the total number of bubbles present at any time, first increases with time, and then becomes time invariant. It increases as more and more bubbles are nucleated and reaches a constant value when nucleation stops. With an increase in freon percentage, for a fixed $W_{W,0}$, we obtain somewhat lower total number of bubbles as the peak of nucleation rate is lower while the interval of nucleation is not much different to compensate for the lower maximum value.

Third moment ($f_3 V_L$) profile, which is a measure of total volume of bubbles, is shown in Figure 10. With increase in Freon percentage, though the number of bubbles decreased, higher evaporation rate led to formation of larger bubbles and, thus, higher $f_3 V_L$.

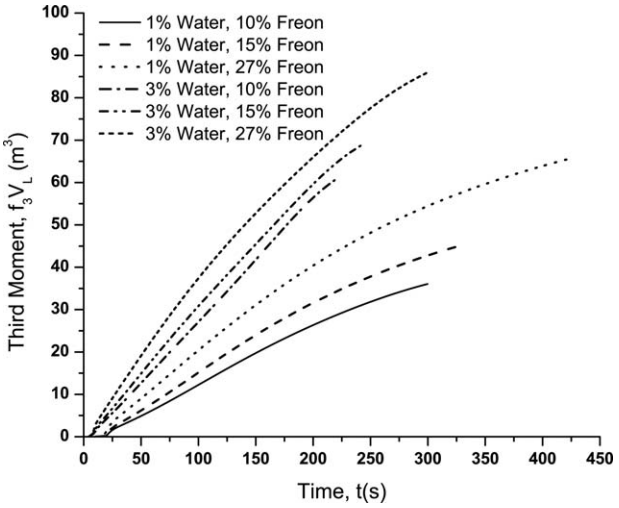

Figure 10. Variation of third moment with time.

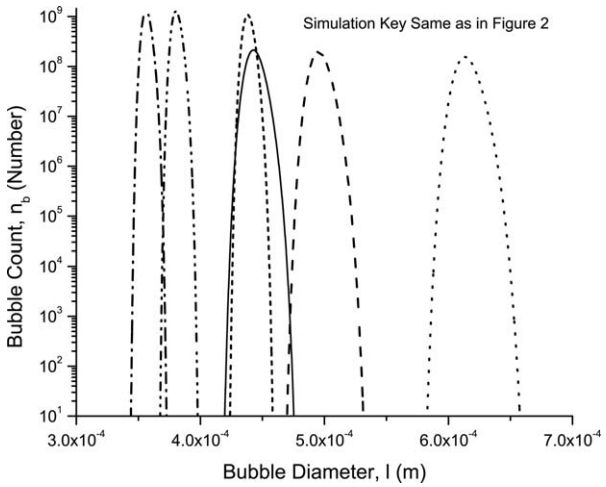

Figure 12. Variation of bubble count with size.

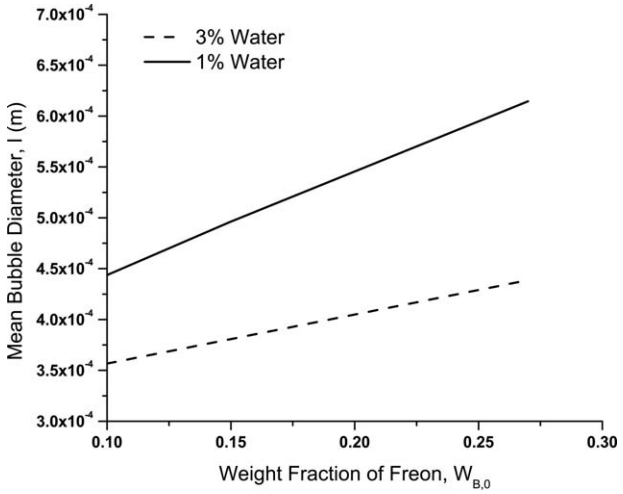

Figure 13. Variation of mean bubble size with initial freon concentration.

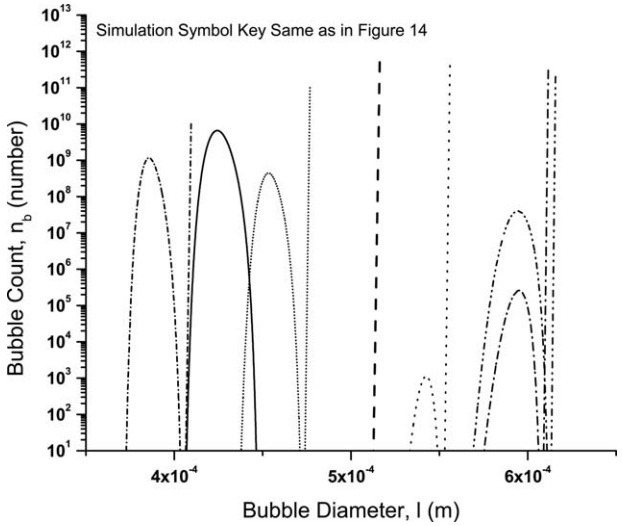

Figure 15. Variation of bubble count with size for different initial nuclei counts.

Foam Density

The change in overall foam density, ρ_{all}, with time is shown in Figure 11. As the evaporation and degassing begin after some period of time, overall density starts to fall down only after some finite time. The density of foam stops decreasing any further after gelation occurs. The simulation of the model proposed by Baser and Khakhar[8] shows poor agreement at an earlier period of time. This is because they allow only CO_2 and not freon to be transferred into the gas phase till the boiling point of the mixture is reached. Therefore, the decline in density predicted from their model is much slower than what was observed in experiments. Once the boiling point of freon is reached, it is allowed to suddenly evaporate, in their model. This causes a kink in the density profile calculated by them. In this model, both freon and CO_2 are evaporating/diffusing to the gas phase from the beginning of nucleation. Thus, the simulation curves are smooth and follow the experimental points better. Mass-transfer rates seem to be underestimated in this model and can be attributed to neglect of convection. It is known that even the slightest relative movement between bubbles and liquid increases mass-transfer rates when Schmidt number is large.

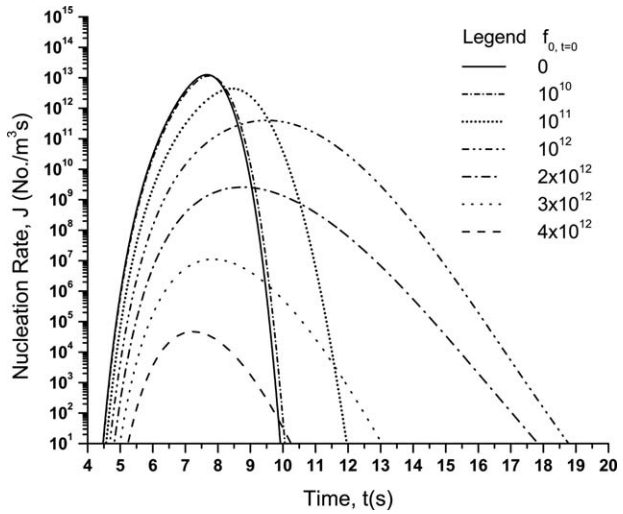

Figure 14. Variation of nucleation rate with time for different initial nuclei counts.

Calculations for various formulations show that with the increase in total amount of blowing agent, we obtain a higher density, as expected from the profile of third moment in Figure 10. This is counter intuitive, as one would expect lower density with higher amount of both the blowing agents, and the trend is predicted by this model.

Bubble-Size Distribution

In Figure 12, bubble count, n_b is plotted against bubble size. Bubble size increases with time. The bubbles that are born at the inception of nucleation are the biggest and bubbles born near the end of nucleation period constitute the population of the smallest bubbles. With an increase in the nucleation period, the difference in the age of the bubbles increases and we get a broader distribution. In Figure 12, for $W_{W,0}$ equal to 3%, it is seen that the distribution is narrower which can be attributed to smaller nucleation period. There are other complicating factors as well that affect the bubble-size distribution. The driving force for mass transfer of CO_2 first increases with time and then decreases as generation of CO_2 declines. The same is true for freon also. Initially, the bubbles are CO_2 filled and hence, driving force for mass transfer is greater. As production of CO_2 declines, the bubbles tend to have more and more freon, and the driving force for its transfer also reduces. Conversely, the surface area for mass transfer increases with time. Bubble growth is, therefore, an outcome of these opposing effects. Complex interplay of these competing factors gives rise to the final bubble-size distribution.

Mean Bubble Size

Calculations also show that the mean bubble diameter increases with increase in freon percentage as there is more freon to evaporate (Figure 13). As discussed before, an increase in water percentage, which generates more CO_2, produces increased number of nuclei. Although more CO_2 is generated which also needs to be contained in bubbles, an enormous increase in number of nuclei well compensates for extra CO_2, and for a fixed freon percentage

the mean diameter is reduced significantly. It can be seen that addition of water does offer some control on bubble size. As mentioned in the introduction, however, one has to note that coalescence does increase the bubble size.

Effect of Incorporation of Gas Nuclei

The final bubble-size distribution in the foam is decided by the rates of nucleation and growth. The incorporation of a chemical blowing agent generating CO_2 provides a method of modifying the bubble-size distribution. The incorporation of gas nuclei in the reaction mixture provides another method, which can modify the rates of nucleation drastically by reducing supersaturation through bubble growth. Such nuclei can be present in the reaction mixture as tiny bubbles or leakage of gas. The effect of incorporation of nuclei from outside was, therefore, investigated. Figure 14 shows the rate of nucleation as a function of time, where the extra gas has been added in the form of nuclei. It is seen that with the increase in initial nuclei count ($n_{b,0}$) (with diameter of 0.4 μm), the rate of homogeneous nucleation falls drastically. At $n_{b,0}=4\times10^{11}$, the rate of homogeneous nucleation is reduced drastically and for 5×10^{11} it is negligible. Thus, the bubble-size distribution now is virtually independent of the rate of homogeneous nucleation. This is clearly seen in Figure 15, where number of bubbles is plotted versus bubble size. Without addition of gas, the bubble size varies over a range but for addition of nuclei count $n_{b,0}=5\times10^{11}$, the bubble size is uniform, because nearly all bubbles start growing at the cream time. Thus, addition of nuclei from outside can in principle offer a powerful method of controlling bubble-size distribution.

CONCLUSIONS

The use of a chemical blowing agent modifies the dynamics of foam formation by changing the rate of nucleation significantly. The addition of higher initial quantity of water raises the rate of rise of temperature of the foaming liquid because the reaction is exothermic and first order with respect to water. The freon not only reduces the rate of reaction by dilution but also reduces the rate of rise of temperature because of its evaporation into the bubbles.

The CO_2 concentration in the liquid passes through a maximum with time, because of CO_2 generation, nucleation, and mass transfer. The model predicts that the time over which nucleation occurs decreases with increase in water content. The model also makes a rather unexpected prediction, that for the same water content, the period of nucleation decreases with increasing freon content. Thus, the addition of chemical blowing agent offers a technique to partially control the bubble-size distribution.

Addition of nuclei from outside in the form of microbubbles can result in drastic reduction in homogeneous nucleation and can result in bubble-size distribution controlled mainly by original bubble-size distribution and mass transport to them.

NOMENCLATURE

A_{OH}	frequency factor for polymerization kinetics, m^3/k eqiv/s
A_W	frequency factor for isocyanate-water reaction kinetics, s^{-1}
Ant A	Antoine constant, N/m^2, K
Ant B	Antoine constant, N/m^2, K
Ant C	Antoine constant, N/m^2, K
B	frequency factor of gas bubbles joining the nucleus, s^{-1}
C_B	concentration of freon in bulk liquid, k mol/m^3
C_{NCO}	initial concentration of NCO end group in bulk liquid, k equiv/m^3
C_{OH}	initial concentration of OH end group in bulk liquid, k equiv/m^3
C_W	concentration of water in bulk liquid, k mol/m^3
C_{CO_2}	concentration of CO_2 in bulk liquid, k mol/m^3
$C^*_{CO_2}$	concentration of CO_2 at bubble-liquid interface, k mol/m^3
C^*_B	concentration of freon at bubble-liquid interface, k mol/m^3
ΔC_B	$(C_B-C^*_B)$, k mol/m^3
ΔC_{CO_2}	$(C_{CO_2}-C^*_{CO_2})$, k mol/m^3
C_{p_B}	specific heat of freon in liquid phase, J/kg.K
$C_{p_{B,g}}$	specific heat of freon in gas phase, J/kg.K
$C_{p_{CO_2,g}}$	specific heat of CO_2 in gas phase, J/kg.K
C_{p_p}	specific heat of polymer and prepolymer, J/kg.K
D	diffusion coefficient, m^2/s
E_{OH}	activation energy for polymerization kinetics, J/k mol
E_W	activation energy for isocyanate-water reaction kinetics, J/k mol
$f(l)$	number density function of bubbles in the size range l to $l+dl$, /m^4
f_nV_L	nth moment of bubble-size distribution, m^n
ΔF^*	minimum free energy change for the formation of critical nucleus (classical nucleation theory), J/k mol
G	growth rate of bubbles, m/s
H	Henry's constant, atm m^3/k mol
ΔH_{OH}	heat of polymerization reaction, J/k equiv
ΔH_W	heat of isocyanate-water reaction, J/k mol
J	nucleation rate, number/m^3s
k	Boltzmann constant, J/molecule.K
K	total number of sets of bubbles, at any instant
k_m	mass-transfer coefficient, m/s
l	bubble diameter, m
l_N	critical nucleus size, m
l_{max}	maximum bubble size, m
m_B	mass of freon in liquid phase, kg
$m_{B,g}$	mass of freon in gas phase, kg
$m_{CO_2,g}$	mass of CO_2 in gas phase, kg
m_p	mass of polymer and/or prepolymers, kg
m_W	mass of water in liquid phase, kg
M	number of molecules of blowing agents/unit volume of polymer solution, number/m^3
M_B	molecular weight of freon, kg/k mol
M_{CO_2}	molecular weight of CO_2, kg/k mol
n	total number of molecules of blowing agents in a critical nucleus
$n_{b,i}$	total number of bubbles in ith set
$N(l)$	mass transfer rate into bubble of size l, k mol/s
$N_{R,i}$	ratio of number of moles of freon to that of CO_2 in the vapor phase of ith set of bubbles
P	pressure, N/m^2

P_L	pressure in the liquid phase, N/m^2
P^{sat}	saturation vapor pressure of freon, N/m^2
P_V	vapor pressure of the liquid phase, exerted by freon and CO_2, N/m^2
P_{V_B}	vapor pressure of freon in the liquid phase, N/m^2
$P_{V_{CO_2}}$	vapor pressure of CO_2 in the liquid phase, N/m^2
R	gas law constant, J/k mol.K
r	point marking the beginning of a characteristic
t	time, s
Δt	time step of numerical integration, s
t_c	cream time, s
t_{gel}	gel time, s
t_r	rise time, s
T	temperature, K
T^*	boiling point of the solution, at atmospheric pressure, K
V_L	volume of the liquid phase, m^3
W_B	weight fraction of freon
W_B^*	weight fraction of freon at gas–liquid interface
$W_{B,N}^*$	weight fraction of freon in a bubble nucelus at gas–liquid interface
X	fractional conversion of reactive species
$X_{OH,gel}$	chemical conversion of polyol to gelation
$y_{B,i}$	mole fraction of freon in *i*th set of bubbles
$y_{B,N}$	mole fraction of freon in the nuclei
$y_{CO_2,i}$	mole fraction of CO_2 in *i*th set of bubbles

Greek letters

γ_B	liquid phase activity coefficient of freon
λ	latent heat of vaporization of freon, J/kg
ρ_{all}	overall foam density at gel point, kg/m^3
ρ_B	density of the freon, kg/m^3
ρ_L	density of the liquid phase, kg/m^3
ρ_p	density of polymer and prepolymer, kg/m^3
ρ_W	density of water, kg/m^3
σ	surface tension, N/m

Subscripts

o	initial condition
B	blowing agent, freon
CO_2	carbon dioxide
g	gas
i	index of a set of bubbles
L	liquid phase
N	bubble nucleaus
OH	polyol
p	polymer, prepolymer
W	water

REFERENCES

1. Woods, G. The ICI Polyurethane Handbook; Wiley: New York, **1990**.
2. Oertel, G. Polyurethane Handbook; Hanser: New York, **1993**.
3. Klempner, D.; Frisch, K. C. Handbook of Polymeric Foams and Foam Technology; Oxford University Press: New York, **1991**.
4. Gibson, L. J.; Ashby, M. F. Cellular Solids; Cambridge University Press: New York, **1997**.
5. Lim, H.; Kim, E. Y.; Kim, B. K. *Plastics, Rubber Comp.* **2010**, *39*, 364.
6. Tesser, R.; Di Serio, M.; Sclafani, A.; Santacesaria, E. *J. Appl. Polym. Sci.* **2004**, *92*, 1875.
7. Hawkins, M. C.; O'Toole, B.; Jackovich, D. *J. Cell. Plast.* **2005**, *41*, 267.
8. Baser, S. A.; Khakhar, D. V. *Polym. Eng. Sci.* **1994**, *34*, 642.
9. Rojas, A. J.; Marciano, J. H.; Williams, R. J. *J. Polym. Eng. Sci.* **1982**, *22*, 840.
10. Marciano, J. H.; Reboredo, M. M.; Rojas, A. J.; Williams, R. J. *J. Polym. Eng. Sci.* **1986**, *26*, 717.
11. Niyogi, D.; Kumar, R.; Gandhi, K. S. *AIChE J.* **1992**, *38*, 1170.
12. Shutov, F. A. *Adv. Polym. Sci.* **1983**, *51*, 155.
13. Niyogi, D.; Kumar, R.; Gandhi, K. S. *Polym. Eng. Sci.* **1999**, *39*, 199.
14. Jung, H. C.; Ryu, S. C.; Kim, W. N.; Lee, Y. B.; Choe, K. H.; Kim, S. B. *J. Appl. Polym. Sci.* **2001**, *81*, 486.
15. Kim, Y. H.; Kang, M. J.; Park, G. P.; Park, S. D.; Kim, S. B.; Kim, W. N. *J. Appl. Polym. Sci.* **2012**, *124*, 3117.
16. Seo, W. J.; Jung, H. C.; Hyun, J. C.; Kim, W. N.; Lee, Y. B.; Choe, K. H.; Kim, S. B. *J. Appl. Polym. Sci.* **2003**, *90*, 12.
17. Li, M.; Huang, X.; Liu, H.; Liu, B.; Wu, Y.; Xiong, A.; Dong, T. *Fluid Phase Equilib.* **2013**, *356*, 11.